

Analysis and reproduction of the frequency spectrum and
directivity of a violin.

by Rik VOS

Institut de Recherche et Coordination d'Acoustique/Musique
Paris, France

Supervisors: O. WARUSFEL and N. MISDARIIS

January 2003

0.1 Words of Gratitude

As the supervisor of my internship at Ircam I thank Olivier Warusfel for the opportunity to be part of the team of IRCAM. I thank him also for the nice, helpfull and pleasant meetings and his remarks and ideas on the subject.

I thank Nicolas Misdariis for all our hours of discussing the subjects, which helped a lot in my understanding of the problems and solutions. His remarkable sense for overview and physical interpretations kept the research right on track. I wish him all the luck and fine moments in the further work on musical instruments.

Furthermore, although René Caussé was not the direct supervisor, I earn him a lot for his knowledge of instruments, and all that happens in the field of acoustics. I thank him as well for all the times he wanted to listen to the research troubles encountered.

I thank Patricio De La Cuadra, Eric Hubert, Brian Katz, Magali Deschamps, André Almeida and Gérard Bertrand for the nice time spent in Labo7 with fun, tales, discussions and all the language problems. Good luck to you all!

Furthermore, much thanks to Alain Terrier for all the work and time preparing the measurement and calibration setup, and all his ideas about them. His golden hands are incomparable.

Last but not least, I thank the people who I did not see all day, but made the time spent at IRCAM a pleasant time: Joël Bensoam, Nicolas Ellies, Christophe Vergez, Guillaume Vander-noot, Sylvie Benoit and Ghislaine Montagne.

Abstract

The violin has been the topic of a lot of research over the past few hundred years. Its characteristic sound has, during live performances, not a omnidirectional radiation, but a radiation pattern dependent on the frequency. Those rays of sound, for higher frequencies, 'enlighten' the acoustical properties of the surrounding, giving an extra dimension to the live performance. The goal of this research is to study this frequency dependent sound radiation and to synthesize this directivity behaviour.

The model of the violin is a 70 year old violin, whose sound field is measured. This is not done the direct way, where the bridge is excited and its radiation is measured, but the inverse way, where an external source excites the violin from a certain direction. The vibrations of the violin are then captured by a calibrated sensor inside the bridge. Those measurements use the reciprocity assumption, which states that if the body vibrates strongly due to a sound wave with given frequency and direction, it will radiate sound waves with the same power and direction as this excitation. Those measurements are done at the anechoic chambre at IRCAM, over a large frequency range and over a whole sphere surrounding the violin.

From the literature is known, that the violin will have standing wave solutions of the vibrations of its physical structure. The analysis consists of finding the peaks in the measured power spectrum, which are assumed to appear at the modal frequencies of the body. The width of the peak defines the damping coefficient of this mode. Per mode, the radiation pattern is decomposed into the zeroth and first order spherical harmonics, yielding an estimated directivity of the sound.

The reproduction is based on the propagation laws. If we have two sources whose sound field are equal at a surrounding surface, the sound fields outside this surface are the same according to the propagation laws. In our case, the first source is the violin and the second is a unit which can generate elementary directivity patterns using the zeroth and first spherical harmonics. Now, the decomposition of the radiation patterns can be used directly as multiplication factors in the field reproduction.

To reproduce the sound of the violin, a modal-based synthesis program is used, which decomposes complex structures in simple structures having vibrating modes. Those modes interact together when excited, and the velocity of the modes at a given position in the structure is the output sound. This program is extended with a directivity processing function.

In this research the measurements, analysis and reproduction are all done. There are three main problems encountered. The first is, that the peak and damping finding algorithm are too straightforward, which result in large differences between the simulated and real frequency spectrum. The second is, that high frequencies dominate the power spectrum in the measurements. These give very sharp sounds during the reproduction phase. The last is, that the Fourier decomposition returns complex factors, meaning phase shift information. In a signal processing sense, these phase shifts result in filter operations. This is left for further research.

Contents

0.1	Words of Gratitude	1
1	Introduction	3
1.1	Background	3
1.2	History	3
1.3	Other groups in the world	4
2	Theory	5
2.1	Wave equation and solutions	5
2.2	Body vibrations and modes	6
2.2.1	Undamped string	7
2.2.2	Damped string	7
2.2.3	Remark on modal shapes and bending a string.	8
2.3	Sound field reproduction	9
2.3.1	Actuator based	10
2.3.2	Spherical harmonics based	10
2.3.3	Direction based	11
2.4	Error reduction methods	11
2.5	Fourier spatial decomposition	12
3	Measurements of the violin body resonances	13
3.1	Goal and main setup	13
3.2	Radiation principles	14
3.3	Sensor choice	15
3.4	Sensor Calibration	15
3.5	Measurement setup	15
3.5.1	Source	17
3.5.2	Environment	17
3.5.3	Reference microphone	18
3.6	Reproducibility	18
3.7	AMS software	18
3.8	results	19
3.8.1	Raw measurements	19
3.8.2	Sensor	20
3.8.3	Setup	20
3.8.4	Further research	21
4	Analysis	22
4.1	Matlab toolbox	22
4.2	Finding peaks and losses	22
4.2.1	Description	22

4.2.2	Discussion	23
4.3	Finding directivity	24
4.4	Spherical harmonical decomposition	25
5	Reproduction	28
5.1	Modalys	28
5.2	Violin modelling	28
5.3	Connection of Modalys with La Timée	29
5.3.1	Modal based	29
5.3.2	Other methods	29
6	Conclusions and future work	31
6.1	Conclusions	31
6.1.1	Measurements	31
6.1.2	Analysis	31
6.1.3	Reproduction	32
6.2	Future work	32
6.2.1	Complex reproduction	32
6.2.2	More instruments	32
6.2.3	Rotating violin	32
6.2.4	High frequency behaviour	32
7	Social report	34

Chapter 1

Introduction

1.1 Background

Imagine, you are a music performer with bright ideas about combining odd, but very sophisticated sounds with a traditional, but excellent orchestra. Imagine on the other hand, you are a scientist who has build a six-way loudspeaker box which can beam sound in different directions. The combination of both fields you just imagined is the field of interest in this research done at IRCAM, "Institut de Recherche et Coordination Acoustique/Musique", at Paris, France. Here, artists and scientist are working together to fuse science and arts.

The forlying report deals with the reproduction of the sound made by a violin. In this case, sound is not just a signal in time, which can be played over loudspeakers at home, but the full 3D representation of the sound pressure radiated by the violin. The difference is remarkable: where a real-life violin beams its sounds as if they were coming from a well-known discoball, the sound played by a loudspeaker has a dry, non real effect. The effect of playing the sound through one loudspeaker is clear: sounds are spread by the directivity of the loudspeaker, which has a totally different radiation pattern than the violin one.

One of the solutions brought up by Ircam was to build a loudspeaker box which can radiate sounds in various directions with a very precise control. This device is called La Timée, and is able to reproduce an acoustical monopole and dipole in all three spatial dimensions in a large frequency range.

The sound itself is synthesized by the program Modalys, which simulates instruments by modal decomposition of the structure. It uses simple structures, like strings and plates. Those structures interact with each other only through interaction between their modes. This method is called modal-based, as a structure can only vibrate in a linear sum of its modes.

This research is done as an internship as part of the Master course in Applied Physics, Delft University of Technology, The Netherlands. It took place at Ircam, Paris, France.

1.2 History

The modal approach of instruments was founded a long time ago, 25 years ago [4], but only after the huge improvement of computer speed and availability it was made possible to implement. So, starting 1988 by Jean-Marie Adrien, at Ircam, one of the first implementations of the modal approach was made [3]. The first software, called Mosaïc, used some basic objects like plates, tubes, strings and two-mass systems. This program, first for MacOS and later for Linux as well, is the base of Modalys, which is the name nowadays. A graphical front-end for MacIntosh made the program easier to use for artists.

The directivity control was studied by Philippe Dérogis, who tried to approximate an or-

dinary wavefield with a limited number of loudspeakers [6]. Here, there are two sound fields: one of the object which we try to simulate, and the other which is the result of the synthesis. The main idea is now, that if the sound pressure field on a surface surrounding the synthesis field equals that of the original field, there will be no difference between the fields outside this surface. This is a result of the propagation laws. As the synthesis loudspeakers will in general never form a base of the real field, the matching of the two fields will always be an estimation. In practice, this estimation will be a fitting algorithm which yields the filters for the subsequent loudspeakers.

Nowadays, the setup is slightly different, as the input to the system should be already divided into four independent signals: one for the (direction-independent) monopole and the three dipoles. Using phase shifts and amplitude variations between these four signals, the sound can be radiated from perfectly monopole to perfect dipole in any angle. Again, a simple user interface has been implemented for MacIntosh.

1.3 Other groups in the world

In 1995, at the Helsinki University of Technology, a trumpet and guitar are modelled [7]. Here, a looped delay line is used with end filters to model the modes. This setup will automatically yield resonance frequencies. They reproduced the sound radiation using digital filters, though these were only frequency dependent. Outputting every mode with its own directivity, they found too costly in computational time for real-time applications.

Starting the end of the 70's, the group of Gabriel Weinreich at the University of Michigan has done a lot of acoustical experiments and theory on the violin [8], [9], [10], [11]. There has been inter-institutional co-operation with Ircam in 1984 and 1991. Most of the preliminary work and thoughts on the measurement of the directivity of a violin are based on his articles. The method they used was putting a violin in a sound field with plane waves, and measure the vibrations of the bridge absolutely, i.e., with respect to the suspension of the violin. Nowadays, Prof. Weinreich is retired, and the University of Michigan has left the field of acoustical physics.

The Laboratoire d'Acoustique Musicale de l'Université Jussieu, also in Paris, studies the modal shapes of the violin and its directivity. They propose an array of loudspeakers to beam the sound to one spot on the violin, and measure its resulting vibrations [16].

Chapter 2

Theory

2.1 Wave equation and solutions

In this section, the basic theory of a sound will be given. As there are a lot of books for the derivation of the basic equations of acoustical waves, we treat them briefly here.

Taking a small cube inside the fluid, we will use two basic equations to describe its movements. The first basic equation is Newton's second law, which states

$$\Delta \vec{F} = \Delta m \frac{\partial \vec{v}}{\partial t} \quad (2.1)$$

where $\Delta \vec{F}$ is the force acting on the small cube, Δm its mass, and $\frac{\partial \vec{v}}{\partial t}$ the acceleration. The second is Hook's law, stating that

$$\delta p = -K \frac{\delta V}{\Delta V} \quad (2.2)$$

where δp is the mean pressure difference inside the cube due to the relative volume change of V and K is the compression modulus.

In first order approximation, meaning that the pressure and velocity inside the cube are constant, combining those two equations yields

$$\nabla^2 p - \frac{1}{c^2} \frac{\partial^2 p}{\partial t^2} = 0 \quad (2.3)$$

where c is the acoustical propagation velocity

$$c = \sqrt{K/\rho_0}$$

with ρ_0 the density of the fluid. In this research, we are dealing with 'normal' acoustical waves, because we deal with regular sound pressures, air and no wind or temperature changes. Therefore, we assume air to be isotropic and loss- and dispersion free.

Now, as we might work with a point source we put equation 2.3 in spherical coordinates. It is seen later on that the solution will be a multiplication of 4 independent solutions,

$$\phi = R(r)U(\theta)V(\varphi)T(t) \quad (2.4)$$

in polar coordinates. Using this information, the wave equation will be

$$\frac{1}{rR} \frac{\partial^2}{\partial r^2} rR + \frac{1}{r^2 U \sin \theta} \frac{\partial}{\partial \theta} \left(\sin \theta \frac{\partial U}{\partial \theta} \right) + \frac{1}{r^2 V \sin^2 \theta} \frac{\partial^2 V}{\partial \varphi^2} = \frac{1}{c^2 T} \frac{\partial^2 T}{\partial t^2}. \quad (2.5)$$

Remark that the left part does not depend on t , neither does the right part depend on φ , θ or r . This means, that eq. (2.5) can be reorganized into two different equations. The first is

$$\frac{1}{c^2 T} \frac{\partial^2 T}{\partial t^2} = -k^2 \quad (2.6)$$

where k is the wave number

$$k = \frac{\omega}{c}$$

with ω the frequency in rad s^{-1} . After some rewriting, the second equation can be again be broken into two pieces, one with only radial dependency, and the other with only angular dependencies. This yields

$$r \frac{\partial^2}{\partial r^2} rR + k^2 r^2 R = n(n+1)R, \quad (2.7)$$

where n is just an arbitrary constant, and

$$\frac{\sin \theta}{U} \frac{\partial}{\partial \theta} \left(\sin \theta \frac{\partial U}{\partial \theta} \right) + \frac{1}{V} \frac{\partial^2 V}{\partial \varphi^2} = -n(n+1) \sin^2 \theta. \quad (2.8)$$

This last equation is called the angular equation, and its solutions are called the Laplace spherical harmonics. Those solutions are in the form [1], [2]

$$S_n(\theta, \varphi) = U(\theta)V(\varphi) = \sum_{m=0}^n [A_m \cos(m\varphi) + B_m \sin(m\varphi)] P_n^m(\cos \theta) \quad (2.9)$$

$$= \sum_{m=0}^n [A_m Y_{mn}^{(1)}(\theta, \varphi) + B_m Y_{mn}^{(2)}(\theta, \varphi)] \quad (2.10)$$

with A_m and B_m complex coefficients depending on the boundary conditions and the orthogonal terms

$$Y_{mn}^{(1)}(\theta, \varphi) = \cos(m\varphi) \sqrt{\frac{2n+1}{2}} \sqrt{\frac{(n-m)!}{(n+m)!}} (1 - \cos^2(\theta))^{m/2} \frac{\partial^m}{\partial \cos^m \theta} [P_n(\cos \theta)] \quad (2.11)$$

$$Y_{mn}^{(2)}(\theta, \varphi) = \sin(m\varphi) \sqrt{\frac{2n+1}{2}} \sqrt{\frac{(n-m)!}{(n+m)!}} (1 - \cos^2(\theta))^{m/2} \frac{\partial^m}{\partial \cos^m \theta} [P_n(\cos \theta)] \quad (2.12)$$

with P_n the polynomials of Legendre,

$$P_n(x) = \frac{1}{2^n n!} \frac{\partial^n}{\partial x^n} (x^2 - 1)^n \quad (2.13)$$

2.2 Body vibrations and modes

In this section, the principle of modal modelling of musical instruments will be described.

As a resonant wave in a body is always a standing wave, a body can only have distinct modes. This thought will be described using an ideal string, but this can be extended to more general shapes.

An ideal string will be divided in small elements. We will apply Newton's law and Hooke's law on every element δx in the string.

An ideal string can have longitudinal and transversal waves, but here we are only considering transversal waves. The reason is, that it is seen that the speed is much higher and losses are larger in longitudinal waves, resulting in non-interesting high frequencies and small contributions in sound. Using the linearity assumption, the longitudinal waves will not effect the transversal waves. So, transversal waves are neglected.

2.2.1 Undamped string

In fact, the derivation of the wave equation is equal as in a fluids, but now transversal waves are defined by its displacement $u(x, t)$. Furthermore, as the transverse waves in x and y orientation are in two different dimensions, they are independent, because all nonlinearities are ignored for now. Now, the equation for every element Δx is equal to the Helmholtz equation in 1 dimension, yielding

$$\frac{\partial^2 u}{\partial x^2} = \frac{1}{c^2} \frac{\partial^2 u}{\partial t^2} \quad (2.14)$$

with standard solutions

$$u(t, x) = A e^{i(\omega t + kx)} + B e^{i(\omega t - kx)}.$$

Using the boundary conditions because of the fixations

$$x = 0 \rightarrow u(0) = 0 \quad (2.15)$$

$$x = L \rightarrow u(L) = 0 \quad (2.16)$$

the solution is the well known standing wave solution for a free vibrating string with fixed edges

$$u(t, x) = A \cos(\omega_n t + \phi) \sin\left(\pi n \frac{x}{L}\right) \quad (2.17)$$

with A a (real) amplitude, ω_n its resonance frequency, ϕ a random factor depending on the displacement at time $t=0$ and n a real integer called the wavenumber. The resonance frequency is determined by filling in eq. (2.14) and working it out, yielding

$$\omega_n = \frac{\pi c n}{L} \quad (2.18)$$

As it is seen, the wave has for a certain n a defined shape and frequency, called modal shape and frequency.

2.2.2 Damped string

To introduce damping, eq. (2.14) will be extended with a damping factor linear to its velocity [12]

$$\frac{\partial^2 u}{\partial x^2} - \frac{1}{c^2} \frac{\partial^2 u}{\partial t^2} - 2\alpha \frac{\partial u}{\partial t} = 0 \quad (2.19)$$

which will, in case the damping is not so much to avoid any vibration totally, alter the solutions to

$$u(t, x) = A e^{-\alpha t} \cos(\omega'_n t + \phi) \sin\left(\pi n \frac{x}{L}\right) \quad (2.20)$$

where ω'_n depends on α via

$$\omega'_n = \sqrt{\omega_n^2 - \alpha^2}. \quad (2.21)$$

As long as the damping is not too much, meaning $\omega \gg \alpha$, then the solution can be thought of as a perturbation of the undamped oscillations. Now, the perturbation theory states, that in first order approximation the shape of the oscillation will remain equal to the non-perturbed shape [14], [17]. In other words, the shape of a mode will not alter by slight damping.

There is one factor which will apply to more general cases, the Q or quality factor. This one is defined to be

$$Q = \frac{\omega_n}{2\alpha} \quad (2.22)$$

but can be understood best in dealing with an external force.

In this case, we extend eq. (2.19) with a external force part, which oscillates at a real frequency,

$$\frac{\partial^2 u}{\partial x^2} - \frac{1}{c^2} \frac{\partial^2 u}{\partial t^2} - 2\alpha \frac{\partial u}{\partial t} = f(x, t) = F e^{\pm i\omega t} g(x) = F \cos(\omega t) g(x) \quad (2.23)$$

where we introduce the shape as a known function $g(x)$, which is not important for the moment. This equation has, due to its linearity, the standing wave solutions

$$u(x, t) = \chi(\omega) F e^{\pm i\omega t} \sin(\pi n \frac{x}{L}) \quad (2.24)$$

where $\chi(\omega)$ is the complex amplitude of the resonating string. Now, filling in this solution in eq. (2.23) yields

$$\chi(\omega) \left(-\frac{\pi^2 n^2}{L^2} e^{\pm i\omega t} + \frac{\omega^2}{c^2} e^{\pm i\omega t} - 2\alpha i\omega e^{\pm i\omega t} \right) = e^{\pm i\omega t}, \quad (2.25)$$

or, with eqs. (2.18) and (2.22)

$$\chi(\omega) = \frac{1}{-\frac{\omega^2}{c^2} + \frac{\omega_n^2}{c^2} - i\omega \frac{\omega}{Q}} \quad (2.26)$$

which is, with normalized frequency $r = \omega/\omega_n$

$$\chi(r) = \frac{c^2/\omega_n^2}{r^2 - 1 - ir/Q} \quad (2.27)$$

This complex fraction can be split into a (real) amplitude and phase,

$$\beta(r) = \frac{1}{\sqrt{(r^2 - 1)^2 + r^2/Q^2}} \quad (2.28)$$

$$\phi(r) = -\arctan\left(\frac{-r/Q}{r^2 - 1}\right) = -\arctan\left(\frac{r/Q}{1 - r^2}\right). \quad (2.29)$$

A plot is given in figure 2.1.

Searching for other ways to define Q , there is one more solution. Here, we search the -3dB points in $\beta(r)$. Using a first order approximation in the square root, assuming $Q^2 \gg 4$, the quality can be defined as

$$Q^{-1} = 2 \frac{\omega_2 - \omega_1}{\omega_n} \quad (2.30)$$

with ω_1 and ω_2 the -3dB points.

This theory can be extended to 2 or 3 dimensions, yielding more complicated solutions but the basic idea of modal shapes, frequencies and forced resonances remains. Furthermore, this theory holds as well for other basic shapes, like a pipe where air is the medium. Here, an open end can be looked upon as a loose end of a string, and a standing wave will appear at or close to its resonance frequencies.

2.2.3 Remark on modal shapes and bending a string.

So, it is seen that a slightly damped string, driven by external forces, can vibrate at all frequencies, but will alter its phase and amplitude at different frequencies. Furthermore, the modal shape defined by the last factor in eq. 2.20 will not change. This might sound a little bit confusing, as in real life something different happens just after a plucked string was letting go. At this very moment, the string will not have a nice sinusoidal form, but a triangular while the external forces are zero. This can only be true as this particular form is a sum over all its modes. As Fourier showed with its fourier series, every shape can be rebuilt by an infinite sum over all its natural frequencies. External forces can only redistribute energy (caught in the amplitudes and phases) over the modes, but cannot change the modal shape.

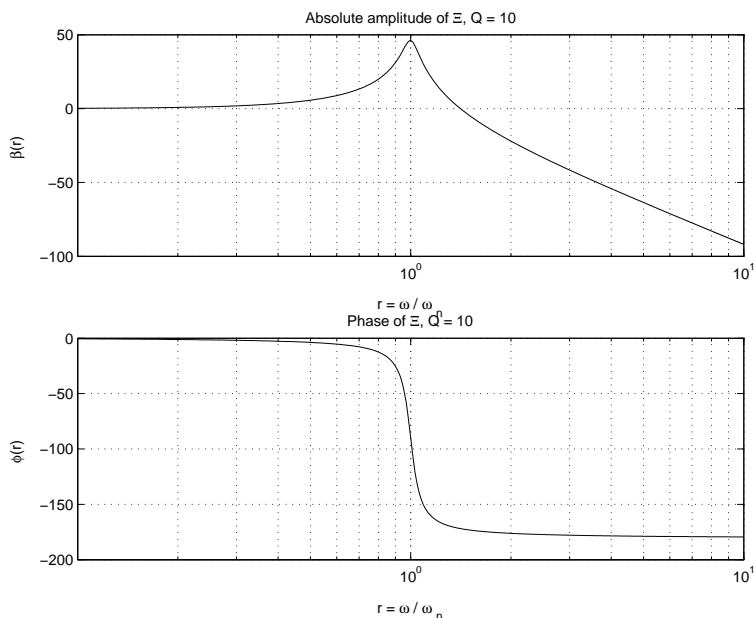


Figure 2.1: Phase and amplitude of forced resonance.

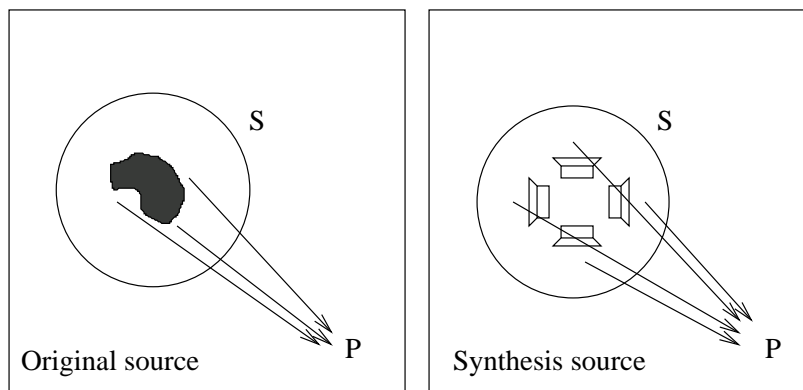


Figure 2.2: Reproduction of the original field: sound field at surface S should be equal

2.3 Sound field reproduction

To make a sound field, multiple actuators are needed. There are various setups possible for this spatial localisation, and the best setup should be fitted to the practical situation. One major choice to make, is whether the actuators are surrounding the listener or are more localized in one spot. The first option can create sound fields that will come from different angles, which will give a large surrounding effect. In the second option, however, the acoustics of the room will filter the played sound more, yielding a natural sound in the room.

If the second method is used, we have to match the produced sound field with the real sound field. Due to the propagation laws of sound waves in fluids, we only have to match the two fields on a given surface surrounding the sources, in order to match the whole field. The schematical representation is given in figure 2.2

2.3.1 Actuator based

Having either of two, a random sound field $T(x, y, z, t)$ has to be reproduced. One of the options which can be used, is measuring the sound field of each actuator and building with this information a new soundfield. In formula, this means

$$\sum_i \alpha_i \cdot P_i(x, y, z, t) = T(x, y, z, t) + \epsilon \quad (2.31)$$

where $P_i(x, y, z, t)$ is the sound field created by every single actuator, α_i a complex factor and ϵ the error made by the reproduction compared to the expected field $T(x, y, z, t)$. If this equation is written a little different, we get

$$\left(T - \sum_i \alpha_i \cdot P_i(x, y, z, t) \right) = \epsilon, \quad (2.32)$$

which states that the ϵ is a measure for the algebraical distance between the reproduction and the original field. As this equation should be solved for every frequency, the α 's will be frequency dependent. In a signal processing way, this means that $\alpha(\omega)$ is a filter which should be applied to the synthesis sources.

See figure 2.3 for the schematic representation of this method.

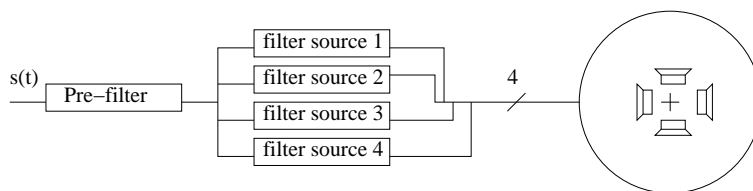


Figure 2.3: Actuator based implementation using specific filters for a directivity pattern

The values of P_i can be found by measurements on the actuators, whereas the α 's can be found by methods which minimize the ϵ in 2.32 (See Sautreau, [1])

One of the main disadvantages in this method is the use of these α 's. As those present the best fit for one given directivity pattern, they should change when we want to introduce another directivity pattern, a rotated one, for example. This would yield a totally different set of filters, which have to be recalculated. Then, they would be implemented one after the other, giving interpolation problems between the two filters.

2.3.2 Spherical harmonics based

A next method, used in La Timée, is to generate elementary directivity through the spherical harmonics. In this case, a set of filters is computed for each spherical harmonic, yielding one bank of filters per loudspeaker. Now, if we want to give a certain directivity to an input signal, we only have to distribute this signal into the bank which has this directivity.

See figure 2.4.

Again, we use 2.31 to describe the field but now the P_i 's are the spherical harmonics. It can be shown (see Nicol [13], p.209) that the number of spherical harmonics depend heavily on the number of actuators. This means in practical applications that the summation will be over a limited number of spherical harmonics. In fact, the used reproduction unit has 6 loudspeakers, which makes it capable of making an omnipole and a combination of the first order spherical harmonics, the 3 dipoles in X, Y and Z direction.

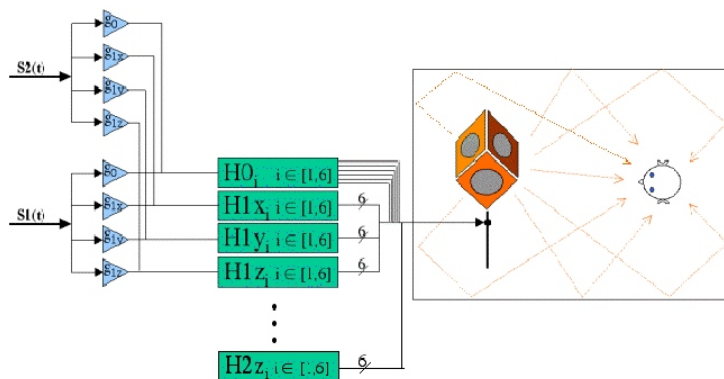


Figure 2.4: New implementation by making fixed filters for first spherical harmonics.

Instead of the previous method, the real advantage of this method lies in the real-time application. Because all filters can be calculated in advance, only the multiplication factors have to be changed to modify the directivity. In practical simulations these multiplication factors are simply gain controls, and easy to implement. The filters themselves can be implemented using dedicated hardware, or smart filtering techniques on a fast computer, and this can be done with care as they don't change anymore.

2.3.3 Direction based

There is one option, we have not worked out very much but might serve as an example. It is the one where we make a large sphere of small loudspeakers surrounding the audience. If we want to let the music come from a certain direction, we put the signal on the loudspeaker which is in this direction.

However, there are some real disadvantages to this method. The first is, that all interference is forgotten. Interferences will play a large role, as we are dealing here with a large amount of actuators, with the same phase and roughly the same amplitude. Second, the wavefield itself is very dependent on the characteristics of the actuators, which will make it harder to rebuild a sound field with great accuracy. Concluding, this method will give some directional effects, but is hard to control and not very scientific. Recall however that the common stereo setup at the cinema has this approach, where the signals of the surrounding loudspeakers might be delayed a little.

2.4 Error reduction methods

Now, several methods can be used for reducing the ϵ . As this one is a function of time and spherical coordinates, and as normal sound will never behave as a simple sum of the first spherical harmonics, there will be no 'best' solution. Some standard fitting methods can be used. Those are:

- Least Squared Error-fit
- Mean Squared Error-fit
- Calculation using spatial Fourier transform
- best directional fit.

This fit can only be in a pre-defined frequency range, which has to be chosen in advance, again depending on the practical situation. Thomas Sautreau has made an analyses of the different methods, see his report [1], so we will not discuss this in detail. He did not work out the Fourier method, this is done by Laborie, [2]. In the next section we will discuss this method in detail.

2.5 Fourier spatial decomposition

If we have a 3D shape on a grid, we would like to decompose this into a set of spherical harmonics, which have its own complex factor.

Here, the calculation of the coefficients is done using the spatial fourier transform,

$$a_{lm} = \int_{\theta=0}^{\pi} \int_{\phi=0}^{2\pi} T(\theta, \phi) Y_l^m(\theta, \phi)^* \sin \theta d\theta d\phi, \quad (2.33)$$

where $T(\theta, \phi)$ is the measured 3D sound field.

The constants a_{lm} will describe the field completely, as long as all indices l and m are taken into account. However, there will be an error in the power spectrum if we truncate these series at a certain level. This can be shown as follows. The spherical harmonics form a orthogonal base, see Laborie [2], p. 18. Now, any pattern can be described by an infinite sum, see equation 2.10 where m goes to infinity. By means of the definition of the Y_{lm} , the total power involved with the coefficients will be

$$P = \sqrt{\sum_{m=0}^{\infty} \sum_{l=-m}^m a_{lm}^2} \quad (2.34)$$

$$= \sqrt{\int_{\theta=0}^{2\pi} \int_{\phi=-\pi}^{\pi} T^2(\theta, \phi) d\theta d\phi}. \quad (2.35)$$

This means, that if we truncate the series at $m = m_{max}$, the power will be smaller as well.

One way to avoid this power loss, we could calculate the power from 2.35, and normalize with this the coefficients a_{lm} . The result will be shown in the measurement chapter.

One other property of this decomposition is the theoretical limit of m_{max} due to the finite grid of the shape. Laborie [2],p. 26, has shown that those limits are

$$m_{max} = \frac{T}{2} \quad (2.36)$$

$$l_{max} = \frac{S-1}{2} \quad (2.37)$$

where T and S denote the number of horizontal and vertical sample points, respectively.

The last point we describe here, is the conversion from complex factors to real values for the dipoles, according to a x,y and z direction. The need for this will become clear at the reproduction phase, here we only give the theory. One of the properties of the coefficients a_{lm} are [2]

$$a_{l,-m} = a_{lm}^* \quad (2.38)$$

which usually states physically that a vector field, in our case the phase propagation of the wave, can go round clockwise or counterclockwise. This gives us the conversion from complex to real values for the first order harmonics,

$$x = \frac{1}{\sqrt{2}} (a_{lm} + a_{l,-m}) \quad (2.39)$$

$$y = \frac{1}{\sqrt{2}i} (a_{lm} - a_{l,-m}) \quad (2.40)$$

$$z = a_{l0}. \quad (2.41)$$

Chapter 3

Measurements of the violin body resonances

3.1 Goal and main setup

One part of this research was the actual measurement of the violin body radiation. For this, we want to measure the radiation for a whole sphere, and the frequency range should be as wide as possible, but at least from a 100 to 2000 Hz. This range was chosen, because Weinreich has predicted and measured the most steady directivity in this range. See Weinreich [9], [11]. Furthermore, he predicted that the field can change every 44 Hz, due to the resolution of resonance frequencies of the top plate and lower plate. Therefore, the frequency resolution should be at most 44 Hz. The angular resolution should be not too large, and Weinreich takes a standard 10° . As we know that some Matlab tools, used for the analysis of the measurements, work well with this angular resolution, we will use this resolution as well.

For these measurements we thought of 2 different ways to measure. The first is the direct way, where we excite the bridge of the violin and measure its resulting sound field with a microphone. The second is the inverse way, where we excite the violin body with an external source and see how much the body vibrates. This second way we call it a 'measurement based on the reciprocity principle', which we will describe in the next section. The main disadvantage of the first method is the excitation of the body. If the violin has to be played by someone, this would introduce large problems for the reproduction of the measurements, as it is very hard to keep a tone very steadily. If the bridge would be excited with an electrical actuator, this will introduce a large unit inside the violin sound field, and a large deformation of the violin itself. Therefore, we use the inverse measurement.

To measure the vibrations of the body, we will use a piezo-electric crystal glued between the violin bridge foot and head. The amplitude of the electric signal will be linear to the force acting between the body and the strings, and this force we will assume to be linear with the amplitude of the body vibrations.

For now, we use only one loudspeaker box as an external source. By doing this, the main uncertainty in the assumption is the fact, that a radiated field from the body has the body as its acoustical center, but the external field has the source as its acoustical center. This uncertainty has to be exploited more, but for this research we will assume no difference in resonances.

To reduce the influence of the characteristics of the loudspeaker, we take a measurement microphone which will capture these characteristics. Afterwards, we filter the measured signal with this reference.

3.2 Radiation principles

Once a body is set in vibration, the soundwaves will radiate. The direction, phase and amplitude in which a mode will radiate, will depend on the modal shape and the frequency of vibration. In other words, the impedance of a certain modal shape and frequency to the medium, air, is most important for the emission or absorption of sound energy. A schematic representation of the system is given in figure 3.1.

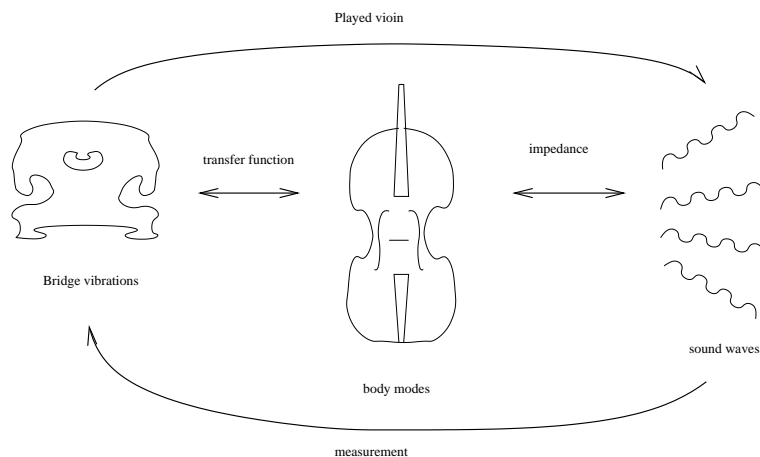


Figure 3.1: Radiation principle and inverse measurement

We assume that the transfer function from the sensor to the body is constant, or at least independent from the frequency. In real life, it will depend on the frequency, but we assume this to be neglectable.

Weinreich [9] gives a deduction of the reciprocity principle. In this article, he uses Newton's third law to demonstrate the effect of interchanging two particles which act a force on each other. This, however, has nothing to do with a question of impedance. We will give an example to demonstrate the difference.

First, we take a small mass with high vibration amplitude, and let this mass set a larger mass in vibration. This larger mass will not have a large amplitude, as its mass will make it slower through $F = m \cdot a$.

Vice versa, if you set the large mass in small vibration, the small mass will (after some time) have a very large amplitude. It does not matter, whether the small mass or the large mass is driven by an external force, the results are the same. This is reciprocal principle, as given by Weinreich.

Now, we take the violin mode vibrations due to a external source. If a small vibration from the external force result in high amplitudes in our violin microphone, we think it is a modal shape. If we would now invoke the reciprocity rule, this should mean that the string should vibrate at a high amplitude to radiate this very frequency; in practice, this would mean that this frequency could hardly be heard.

We can see, that our measurements are based on the adaption of a modal shape to emit or absorb energy, rather than the actual transfer of a force like in a mass-and-spring system. However, this adaptation of the modal shape to transfer energy holds for both ways, absorption and emission, so we could look upon this as the reciprocity principle.

3.3 Sensor choice

As the sensor, we chose a commercially available piezo-electric 'pastille'. It was preliminary its thin size, about 0.7 mm, and its low costs, about 0.5 euro per sensor, which made us choose the one used. From its specifications, we knew that this specific type had a resonance frequency of about 2.3kHz. The hypothesis that this frequency gives the high-frequency bandlimit, due to elastical behaviour, holds as will be seen in the characteristics.

As a reference, and to try, we used also a thin piezo film, which we put underneath the feet of the bridge sandwiched between two copper electrodes. This yielded a three-layer sensor, but which could not be glued due to a limited availability of the film. Therefore, it was very hard to line up the 3 layers underneath the feet which gave a low reproducibility. This caused a large uncertainty in the measurements, and the sensor was not used in the real measurements of the violin.

As a test, we also tried to use a LASER-Doppler 'gun'. This unit outputs the velocity of a surface relative to the gun. But, since we used a force-based calibration setup (discribed in the next section), we could not compare the results. However, it was seen that the LASER was very sensitive to small displacements, and had a lot of noise for higher fequencies. Furthermore, if we would like to use this in our measurements, it gives a lot of problems to keep such a large mass (3.7 kg at IRCAM) in place, and it might give unwanted reflections the sound field. Knowing all this, we gave up the LASER option.

3.4 Sensor Calibration

Both the thin film and the piezo had to be calibrated. For this, we used a vibrating pot and a large contra mass of approximately 3kg, which sandwiched the sensor. See figure 3.2.

The setup itself, including the characteristics of the vibrating pot, was calibrated using an accelerometer put on top of the large mass. An accelerometer is also a small piezo electrical crystal, sandwiched in between a small mass and the vibrating surface. This crystal has a very flat frequency response, and its output voltage is linear to the acceleration of the surface.

Now, putting this sensor on top of the large mass, we assume the transfer function of the large mass to be equal to one, i.e., that the vibrations on top of the large mass are exactly the same as the vibrations at the place of the sensor. We found, however, that the accelerometer picks up a lot of noise, especially above frequencies of 4 kHz. We did not find the reason for this; therefore, these measurements were not used anymore.

The setup using the thin film had a very straight frequency response. Therefore, we assume this film to have a really straight response, so that we could use its signal as a calibration measurement of the setup. Then, we use this calibration to deconvolve the impulse response of our piezo crystal. See for the results figure 3.3.

3.5 Measurement setup

In this section, we describe briefly the setup. More information can be found in the measurement notebook.

As the body, we will take a simple and fairly old violin, a copy of a Stradivarius of 1721. This one was build mechanically between 1920 and 1940, as we were told by a violin builder. The violin is mounted on a metal pipe-and-clamps construction, such that the violin can vibrate as freely as possible in the frequency range of interest, and stays in its place. See the photograph 3.4.

Between the clamps and the violin, small pieces of felt were put to reduce the influence of vibrations of the construction. Furthermore, to reduce the influence of the construction,

Figure 3.2: Calibration setup for the piezo electrical sensor

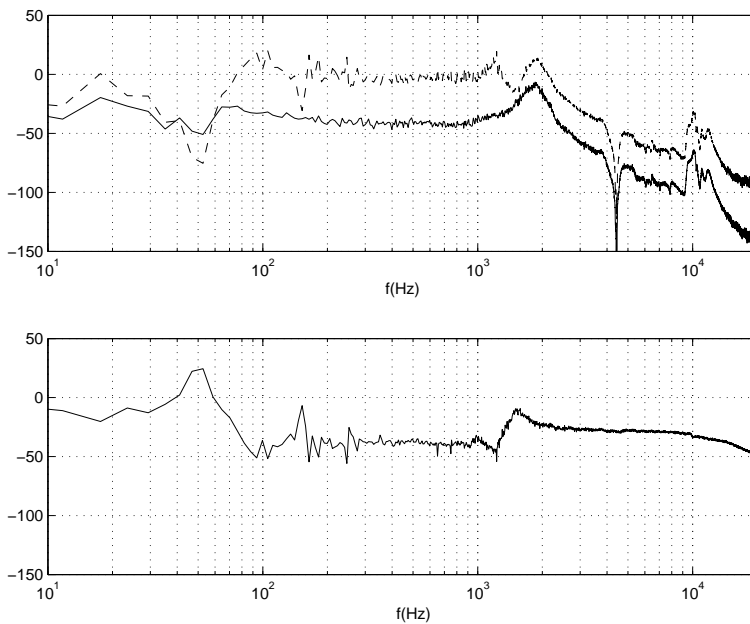


Figure 3.3: Frequency response of the setup. In the upper graph the piezo response without (solid line) or with (dashed line) correction is plotted. The lower graph is the response of the setup measured by the piezo-electric film.



Figure 3.4: Photo of the violin in the anechoic room.

the reference microphone was mounted on the same construction. Now, any resonances of the structure will extinguish as they are captured by both the violin and the reference microphone.

This construction is mounted on a turning table, to assure the 360° angle of measurements in the horizontal plane.

3.5.1 Source

As the source, we have taken a loudspeaker box Tannoy System 600, which has a very flat frequency response over the range of 70Hz to 16kHz, and which has 2-way coaxial loudspeaker configuration. To boost the output of the AMS, we used a standard power amplifier up to a output power of approximately 20W RMS. This power level ensured a sufficient excitation of the violin body, with an overall signal to noise ratio of about 40dB.

The loudspeaker is mounted on an elevation arm, which could make an angle of 135° . This meant that the violin had to be attached rotating over its long axis to achieve a full 180° elevation.

To check the plane wave assumption, and to characterize the loudspeaker and environment, we measured the field with a omnidirectional microphone. The result is given in figure 3.5. For convenience, the frequency axis is in linear scale, to show the phase information more clearly. We see that the phase shift is almost linearly with the frequency, which indicates that we have real plane waves at the position of the violin.

3.5.2 Environment

As we recall, the sound should come from only one direction, which means that no reflections might appear in our measurement environment. We achieved this by placing the setup inside the anechoic chamber, and measured the overall direct to reflection (D/R) ratio. As the turning table is about 70 cm. in diameter, we had to put a damping foam on top of it. Using this, the largest D/R ratio was 28 dB, so a factor of 25, which we neglected in the continuation of our measurements.

Another distorting factor could be the cross-talk, or electromagnetic coupling, between the driving signal and the captured signal. However, we can see the influence of this cross-talk immediately. As the electromagnetic waves have a velocity which is much higher than the velocity of sound in air, we see the cross-talk at the impulse response at times very close ($< 2\text{ms.}$) to zero. We can filter those signals out by starting to read the impulse response for times a little bit more then 2ms.

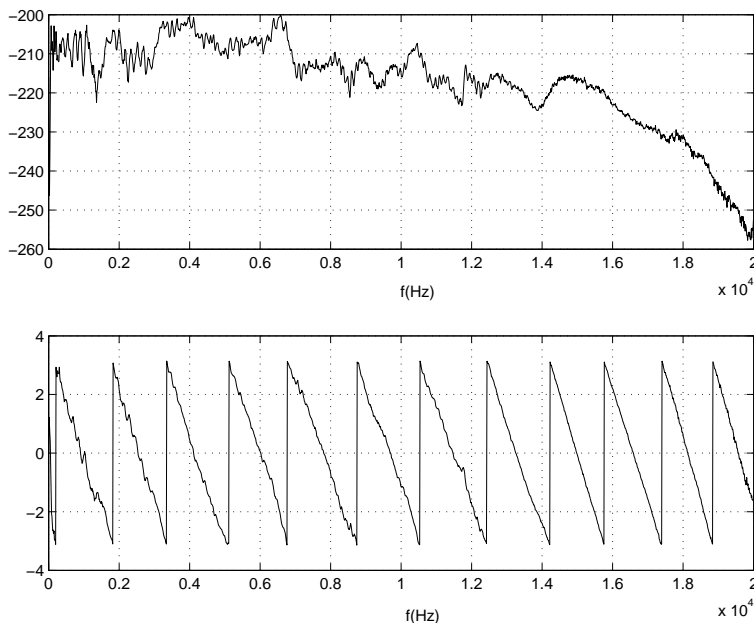


Figure 3.5: Frequency response of the loudspeaker and surroundings, measured with a omnidirection microphone. The x-axis is linear for convenience.

3.5.3 Reference microphone

As a reference microphone, we used a standard electret microphone with known frequency characteristics, a B&K type 2619 with a membrane B&K 4149. This microphone has a frequency response which is flat (± 0.5 dB) from zero to 30kHz for frontal waves. For backward waves it is flat from 0 up to 2kHz, and starting at 2kHz it descends with 10 dB/oct. As we found this too much, we only used the reference values of the frontal sound waves, or more or less frontal. This microphone was mounted on the pipes-and-clamps construction, at exactly the same place as the accelerometer at the violin.

3.6 Reproducibility

To get an idea of the reproducibility of the setup, we measured the whole sphere of the violin twice. The average power absorbed from the source is shown in figure 3.6, where the two curves are allmost the same. It shows only frequencies up to 1 kHz, as the response higher then this frequency is very chaotic, and is not clear on a graph. The third curve is a newer violin, which we measured to see if there would be large differences. Here, we see for low frequencies some large differences. As this violin had a different sensor, placed inside the hole in the bridge. We are not sure this difference is caused by the body vibrations itself.

Here, we see that the overall power spectrum hardly changes due to the suspension of the violin, so we conclude that the suspension does not influence the overall reproducibility of the setup.

3.7 AMS software

The measurements itself were made very easy using the AMS software package, which we describe here very briefly.

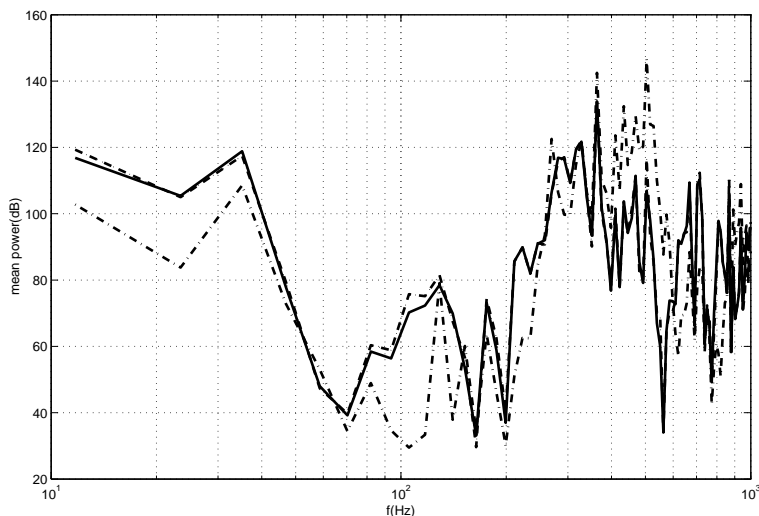


Figure 3.6: Mean power spectrum for 2 violins. Dashed and continuous line are IRCAM violin, the dashed dotted line is newer violin.

	predicted	equal	close	wrong	really wrong
Marshall [18]	27	22	3	2	0
Hutchins [19]	13	7	4	16	5
Knott [20]	11	7	2	18	6
Weinreich [11]	15	15	0	12	3

Table 3.1: Numbers of resonance peaks comparison between violin and literature

This package is an automated measurement tool, which saves the impulse response of a system, or the fourier analyses of this impulse response. For this, it outputs a known wide-range signal and captures the incoming signal through a dedicated card. Using deconvolution of the two signals, the impulse response is calculated and external signals will be averaged, which means in practice that they are almost filtered out. Another advantage of this package is that the AMS software also controls the turning table. This automates the measurements very strongly, minimizing the influence of reading errors by the manipulators.

3.8 results

3.8.1 Raw measurements

To see if the peaks in the power spectrum are really violin resonances, the power spectrum from 100 to 1000 Hz is compared by hand with the modal analysis in 3 different researches. The results are in table 3.1. Here, the first column states the number of resonances predicted by the researchers, the second the number of overlapping peaks, the third the number of peaks which are close to the predicted frequency (less than 25 Hz). The fifth columns states the number of all peaks measured with our violin, which are not present in the literature. The last column states the same, but now only for very distinct peaks in the spectrum.

With those numbers, we feel safe to conclude that we find all modal frequencies of the violin in the measurement results. However, the height of the resonances differ a lot. We assume this to be inherent to the use of different violins, and different measurement methods.

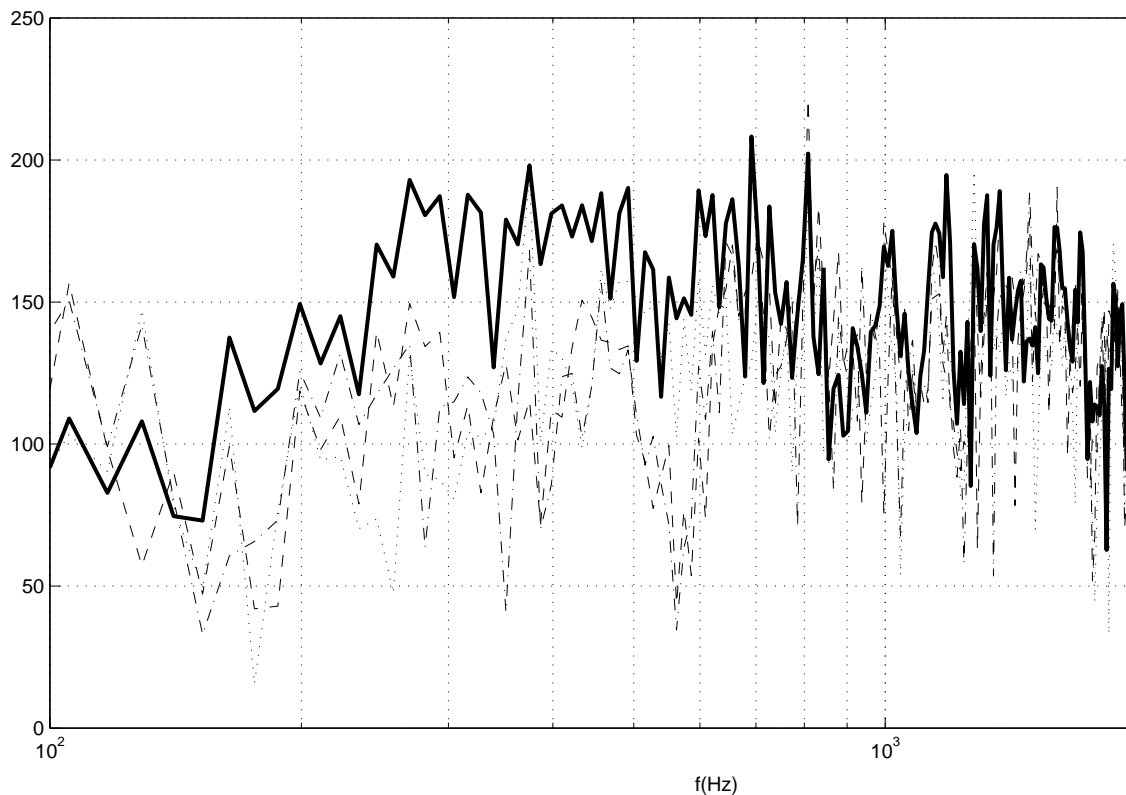


Figure 3.7: Real fourier coefficients of the violin showing its omnidirectional behaviour for frequencies up to 650 Hz. Solid line is the omnidirectional curve, the other three are the 3 dipole coefficients.

Less information can be found over the directivity of the violin, although our violin reacts as Weinreich predicted [11]. He predicts a roughly isotropic sound field below 800 Hz, and more complicated radiation patterns above. Starting 700 Hz, the violin is less omnidirectional, as can be seen in figure 3.7.

To give an idea of the directivity of the violin, four shapes are displayed in figure 3.8. These surfaces connect the points with equal sound pressure.

3.8.2 Sensor

The method used, gives quite accurate the violin resonances. Thanks to the high sensitivity of the piezo sensor inside the bridge we have managed a large signal to noise ratio. However, the calibration of the piezo was not very easy, which we suspect to have introduced some errors in the frequency response of the violin, like the peak at 4.5kHz seen in figure 3.2. Still, the frequency response of the sensor is believed to be very straight between 100 and 1000 Hz, where the first resonances of the body appear.

3.8.3 Setup

The setup was at first sight very sensitive for relatively small displacements of the violin in the setup, but after comparing the two measurements cycles of the violin, the absorbed power was sufficiently equal to reduce the influence of the violin. However, previous test done at IRCAM show that small deviations will occur in real life as well, when the same violin is played by different persons. Therefore, we conclude that our tests are reproducible enough.

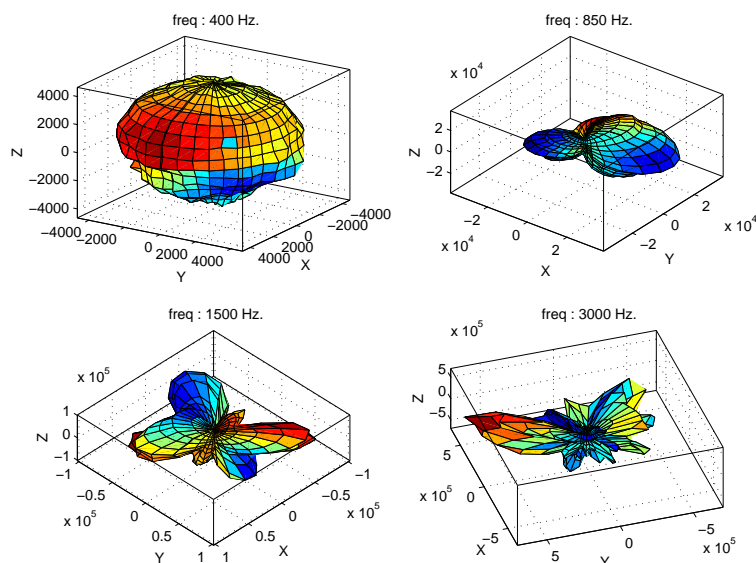


Figure 3.8: Directivity of the violin at different frequencies. The f-holes point towards the x-axis, the fingerboard lies along the y-axis.

3.8.4 Further research

Concerning the measurements method, there is one thing that has to be studied more. We are not sure that if a plane wave hits a flat surface of limited size non-perpendicularly, the exchanged power will not be frequency dependent. The author is aware of the vague description, but was told that this is not so obvious. If this is true, the power spectrum should be compensated with a frequency dependent factor.

Chapter 4

Analysis

4.1 Matlab toolbox

For the reading and processing we used the Matlab Software package, for which a Directivity toolbox was created and the Sautreau toolbox extended. The manual for this toolbox is digitally available with the toolbox software.

The format used to save and process the measurements result is as follows. After reading the .RIF signals into memory, a time fourier analysis is done on the signals. Now, per frequency the fourier coefficients are saved in a matrix, where every element is the (ϕ, θ) position of the violin. This yields a 3D matrix which contains the frequency response of the measured object. Furthermore, the measurement information is saved such as frequency resolution, sample rate, and distance from the source to the measured object.

Now, the toolbox has some specific functions to manipulate the information. The first are the methods to find from the measurements the information needed for the reproduction, which are:

- Finding modes of the violin, the frequency of those modes, and a value which indicates the quality factor Q or the damping.
- Finding the mean absorbed power per mode
- Finding the main directivity per mode

For the found information, there are functions available to show the information in different types of graphs and 3D plots, and a script is made to automate the save the informations in the format needed for the reproduction.

4.2 Finding peaks and losses

In this section we describe the way we filtered from the raw data the different modes. For this, an algorithm has been made, which is quite straightforward.

4.2.1 Description

First, the absolute pressure over all angles at a certain frequency is summed. Here, we take into account the influence of the elevation: for elevations off the equator, the effective surface served by the loudspeaker will be smaller. The summation will yield a mean pressure frequency response, such as 3.6. We assume now, that a mode of the violin body will yield a large resonance in its frequency response, so that we have to find the frequencies of the highest pressure values.

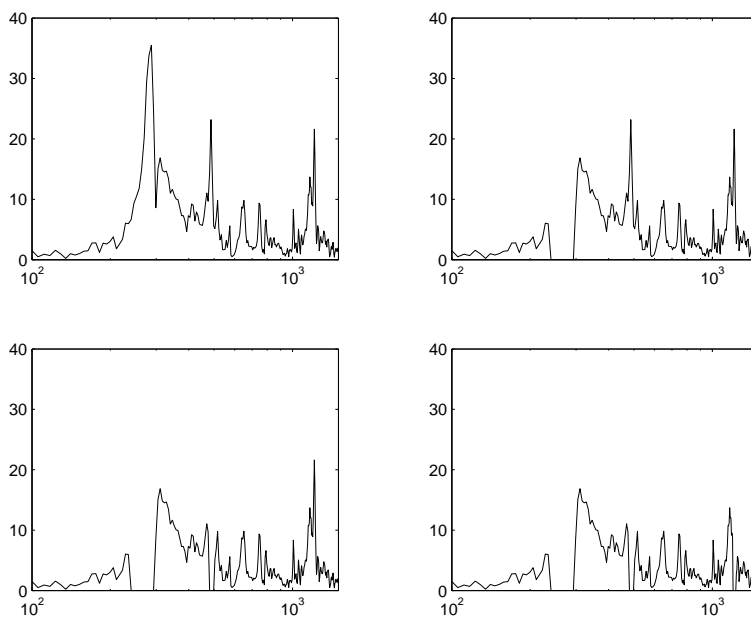


Figure 4.1: Example of the result of the algorithm which finds the center frequencies of the violin resonance.

The algorithm is now, that we search for the highest peak in the spectrum. Once this peak is found, we save the accompanying frequency and erase the peak. This way, we are sure that we will find as much peaks as we want. See for the result, the example graphs 4.1.

Next, we have to find the losses. This is done by finding the -3dB points related to the peak and filling those in in equation 2.30. As the -3dB points will never fit on the frequency grid, the frequency will be interpolated in between the gridpoints.

When the losses and centre frequencies are found, we can fill in equation 2.29 per frequency and plot the summation. See figure 4.2. This is the overall modelled frequency response of the body.

4.2.2 Discussion

As this analysis is quite important for the further reproduction, we discuss the given algorithm.

If we look at the graphs, we see that the higher frequencies (above 3 kHz) have higher amplitudes than the lower frequencies. As the amplitudes at those frequencies can be looked upon as filter characteristics, see graph 4.2, this will give a sort of a band pass filter for high frequencies. In the reproduction phase, this will be heard very strongly. One solution, which is used in the reproduction, is to cut the total frequency range into 3 pieces: one cross-over at 1.5 kHz and one on 4 kHz. Those frequencies are chosen by hand by looking at the graphs, and see where the mean power will be more or less equal over a larger frequency range.

There is also a problem at the low-frequency range. Here, due to the low-region uncertainty of the loudspeaker, the low frequencies are boosted. Again, this will be seen as modes, giving very low frequencies.

Furthermore, if there is a very strong resonance in the violin, for example due to the strings resonating, there will be a sharp peak in the frequency spectrum. This frequency will be heard very strongly in the reproduction phase. The same holds for errors in the calibration of the sensor. If there would be any sharp peaks in the spectrum of the sensor, those will be a mode as well. In other words, the analysis is very sensitive to the measurements, which could be

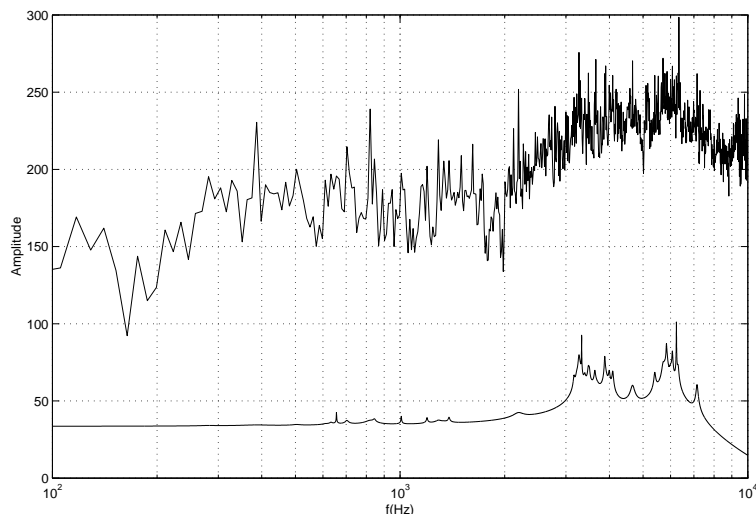


Figure 4.2: Resulting overall resonance of the body. The upper line is the real response, the lower line is the estimation.

expected.

One other feature which were given by the measurements, is the phase information. As can be seen on a amplitude-phase plot, the phase of the body will change very rapidly with frequency. This information is left out of all the analysis, but we do not know the influence of this decision.

One thing, we did not go into deeply, is to find the parameters of the peaks by an analytical fit. One could use equation 2.29, which describes the amplitude and phase of a modal resonance, to use in a Least Squared Error estimation. The problem is, however, that the frequency in 2.29 is in a squared root summation, which will enforce a lot of maths as this will yield non-linear equations. Due to limited time, this option was not worked out any further.

4.3 Finding directivity

After finding the modes and losses per mode of the violin, we have to give every mode its own directivity. As the main goal was to adapt the measurements for the format of La Timée, we were primarily interested in the zeroth and first order spherical harmonics. Though, most of the methods discussed in the section can be used for higher order harmonics.

- By hand

The first method is the most straight forwarded: we plot the measured directivity, and try to fit this by hand with the spherical harmonics. A Matlab function is made to plot the first spherical harmonics. This method yields a lot of work, and is somewhat arbitrarily, though it gives a little insight in the behaviour of the directivity of the violin.

- Fourier decomposition

As was allready described in the theory, the most natural way to calculate the coefficients is to decompose the field into its spherical harmonics using the Fourier theory. The implementation of this method is done by Laborie [2], whose Matlab functions are used in our research.

- Numerical

One way of finding the directivity is by real physical modelling of the violin structure with, for example, a finite element method [19]. This way, the physical shape and material define the modal shape and frequencies, where the shape and frequency predict the directivity of the instrument. However, this method does neither use Modalys for the analysis, nor the measurements, so it does not fit in our research goals.

- Randomized

Here, every coefficient is generated using random numbers. This method will give a spatial sense, but does not use the measurements. It will merely give an idea of the incremented value due to the measurements of the directivity, compared to a non-modal based directivity.

4.4 Spherical harmonical decomposition

In this section, we give the main results of the decomposition.

The first thing, is to check the method of decomposition with equation 2.35, which states that the sum of squared coefficients should equal the total measured power. For this, we calculated the decomposition up to the theoretical limit given by equations 2.36 and 2.37. Then, we calculated the ratio of the measured power to this sums of squared coefficients, see figure 4.3, dashed line. As, maybe due to discretization inside Matlab when calculating the coefficients, this is frequency dependent, we use this ratio to normalize the power spectrum of the decomposition.

Next, we find the influence of the truncation. We plotted again the total radiated power of the violin, this time together with the power resulting from the decomposition in only the zeroth and first order, figure 4.3. Here, we see that up to 2 kHz the pattern can be described with only the zeroth and first order (within range of 3dB), but it falls off for higher frequencies, up to 30 dB at 17 kHz.

We may conclude that for the given setup, the zero and first order approximation will give nice results up to 2 kHz, but the violin starts to generate higher order spherical harmonics above this frequency.

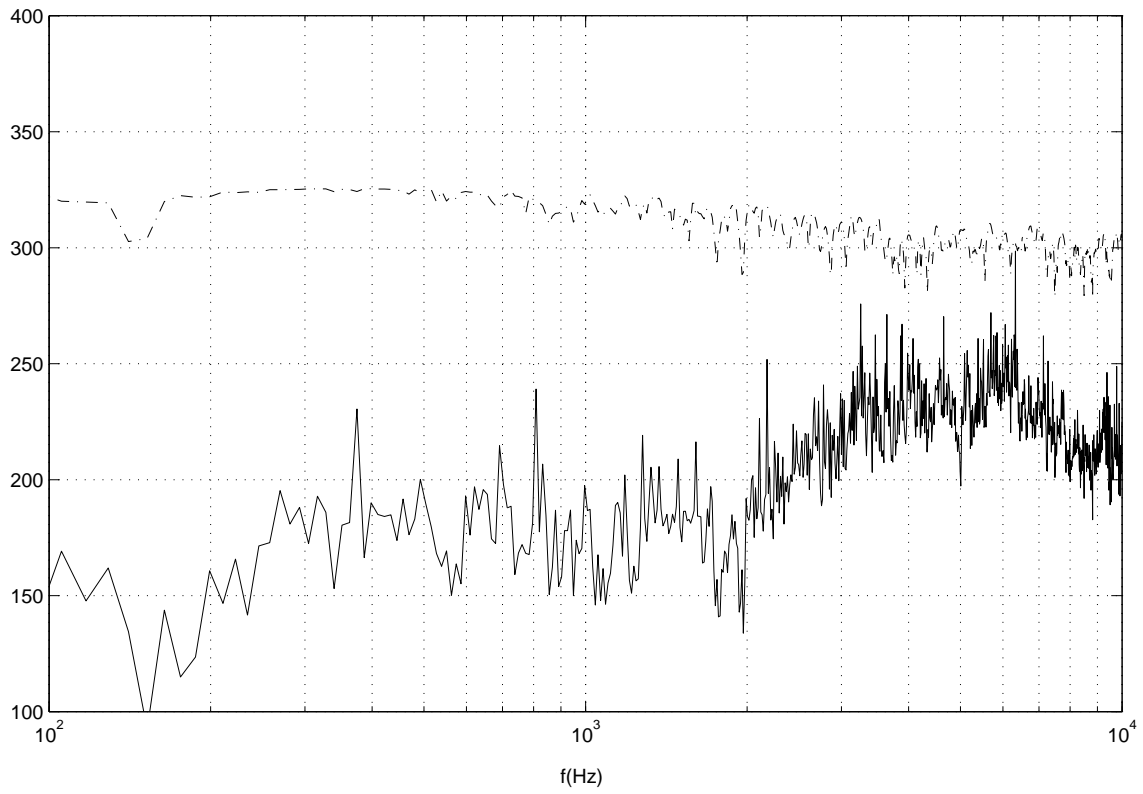


Figure 4.3: The ratio of the measured power and the calculated power of the total decomposition (dash-dotted line). The solid line is the measured power spectrum.

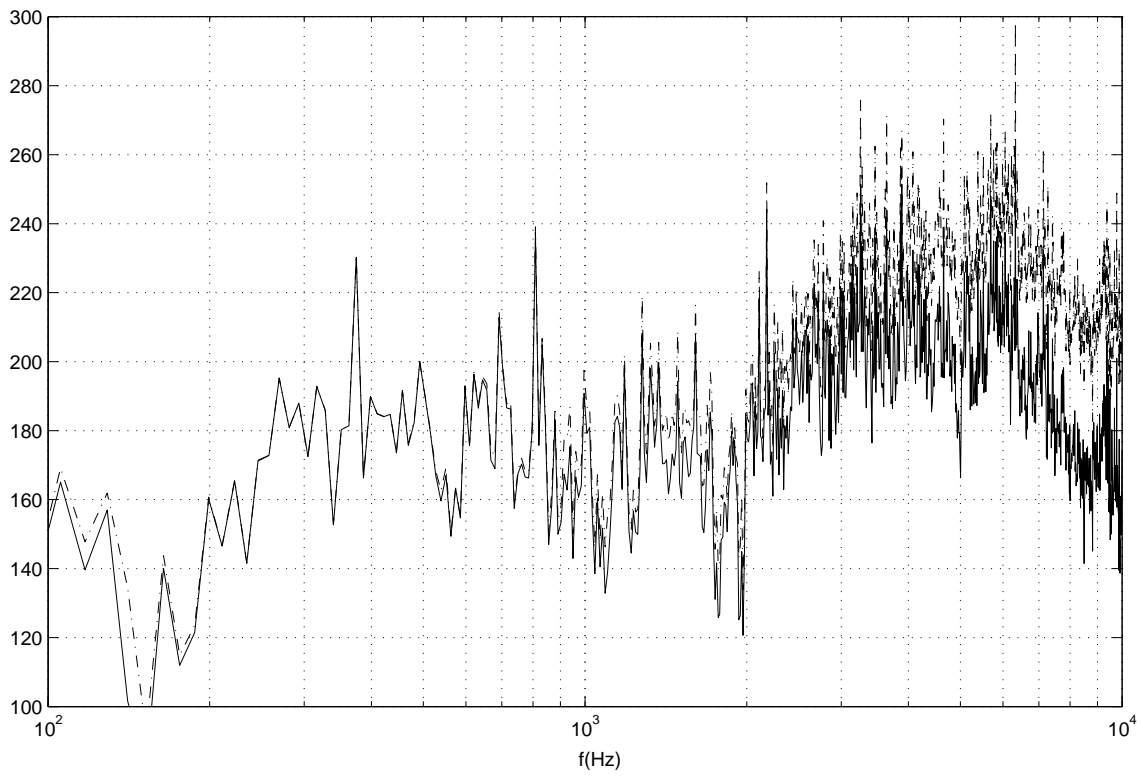


Figure 4.4: Violin power spectrum (dashed line) and the power of the decomposition in only zeroth and first order harmonics (solid line).

Chapter 5

Reproduction

5.1 Modalys

As was already told in the introduction, the software package Modalys is the computational implementation of physical modal principle. In this program, every structure is simulated as a combination of modes, and every mode has its own frequency, energy loss and shape. The frequency and energy loss are just simple numbers, but the definition of a shape in Modalys requires a little explanation. The shape is defined by a number of points, as illustrated in figure 5.1. As is seen, the amplitudes of the shape at equidistant points are taken.

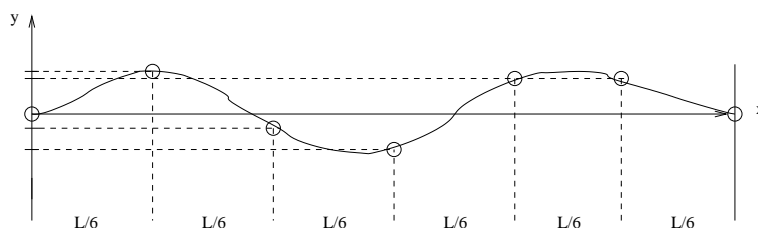


Figure 5.1: The displacement at equidistant points defines the shape in Modalys.

These structures are interacting through predefined connections, such as a violin bridge glued to a plate. User-controlled movements of structures excite the system, such as a bow or a hammer hitting a plate. The output of the simulation is the speed of a structure at a certain point, where the speed is the sum of the speeds of all subsequent modes at this point. To play the sound, a method of saving the files in .aiff format is included in the package. This format is the common format for Linux, and is converted easily into the .au format widely used in the MacOS's. For this research the standard version of Modalys is slightly changed, this will be described in the Chapter Reproduction.

5.2 Violin modelling

To make some sound examples in Modalys, the violin had to be simulated into it. As on a real violin, we took 4 strings, resting on a violin bridge which is glued onto a plate. This plate contains the modes which are to be found from the measurement information.

To play the violin, a bow is used with a standard Modalys bow connection to the strings. This bow connection has a lot of degrees of freedom, making it hard to control: the velocity of the bow, the position of the bow to the strings, and the transversal position of the bow to the

strings, thus setting the force acting on the string. Playing a little with those values yields a very natural sound (but it might as well sound as if the author would play a violin himself..)

The fingers are modelled as small spring-and-mass systems, which press the strings down to a fingerboard. Here as well it is sometimes hard to find the right velocity at which a finger pulls down, but gives a very faint 'tick' as one might hear in real pieces as well. As examples, some staccato played tones are simulated in Modalys as well as a small tango tune.

5.3 Connection of Modalys with La Timée

5.3.1 Modal based

Having the Modalys software and the main directions per mode, we have to process the output of Modalys for La Timée. Recall from equation 2.31 that we had to find the coefficients α_i , which are the coefficients for the zeroth and the first order spherical harmonics of a measured mode. After finding those coefficients, we use them directly to multiply these with the signal coming from our reproduction,

$$W(t) = \alpha_1 \cdot P_M(t) \quad (5.1)$$

$$X(t) = \alpha_2 \cdot P_M(t) \quad (5.2)$$

$$Y(t) = \alpha_2 \cdot P_M(t) \quad (5.3)$$

$$Z(t) = \alpha_2 \cdot P_M(t) \quad (5.4)$$

where $P_m(t)$ is the signal of one Modalys mode.

But, as La Timée has only 4 inputs, we take the orthogonal values of the Fourier decomposition, and forget about the phase part. This will yield an error in the directivity pattern, but the main direction of the dipole will hold.

The output of every single mode in Modalys will be multiplied with the four different factors, giving four different channels, one per spherical harmonic. Per timestep in Modalys this will yield a simple matrix multiplication:

$$\begin{bmatrix} m_1 & m_2 & m_3 & \dots & m_{80} \end{bmatrix} \times \begin{bmatrix} f_{1,1} & f_{1,2} & f_{1,3} & f_{1,4} \\ f_{2,1} & f_{2,2} & f_{2,3} & f_{2,4} \\ \cdot & \cdot & \cdot & \cdot \\ f_{80,1} & f_{80,2} & f_{80,3} & f_{80,4} \end{bmatrix} = \begin{bmatrix} s_1 & s_2 & s_3 & s_4 \end{bmatrix} \quad (5.5)$$

This multiplication does not take too much time in Modalys, and saves a lot of disk space as not all modal velocities should be saved to disk before processing.

The overview of this processing is given in figure 5.2.

5.3.2 Other methods

Although the methods studied in the previous sections are the main results of this research, we will mention some other methods as well to create some directivity.

- Four-output Modalys

As the number of outputs in Modalys can be chosen arbitrarily, one can make four output points in Modalys. Those connection points in Modalys can be put at random places on a plate, which will yield a different balance between the modes per output. This difference in balance will result in some modes with a more omnidirectional directivity, and some with more dipole-like.

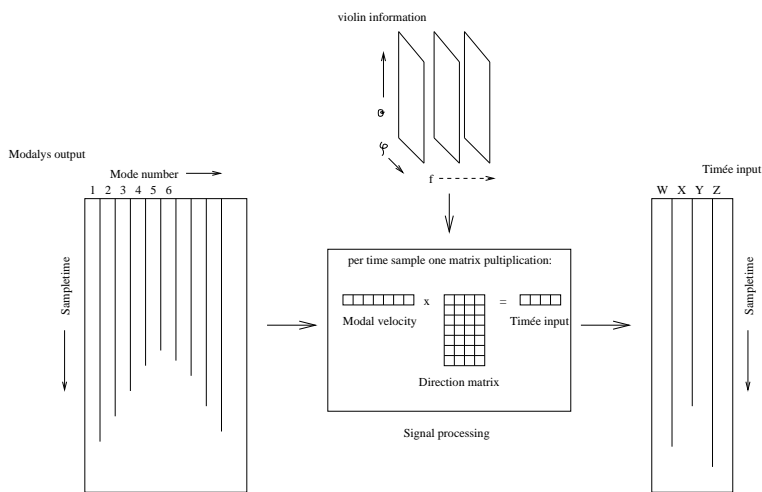


Figure 5.2: Schematic representation of signal processing

- Non-model output

Using a monophonic signal, we could give every frequency its own directivity, using four different filters, one per channel. With this method the modal sounds are not separated. This is already a little bit implemented in La Timée, where the total frequency range is divided into three bands with its own directivity pattern.

Chapter 6

Conclusions and future work

6.1 Conclusions

This research can be split into three parts, the measurements, analysis of the results and the reproduction. Apart from those specific results, the Matlab toolbox for measurements analysis is revisited and extended with directivity analysis functions.

6.1.1 Measurements

As was seen in the chapter, the inverse method of finding the directivity of the violin works very well. The advantage of this method is, that a small sensor inside the bridge is the only disturbing factor from a normal setup, apart from the lack of a real violinist.

The external source, the small size of the sensor and fast computer technology permits us to use high frequencies, where the most fast-changing behaviour of the violin directivity occurs. Nonetheless, in this frequency domain the violin is very sensitive for small suspension changes, which reduces the measurement reproducibility. Furthermore, the sensor calibration was at different circumstances than during the measurements: the calibration mean force was about 30N, but a normal force acted by the strings on the bridge is about 200N [12]. Apart from this, in our measurement the sensor was glued to the two pieces, and during the calibration it was not. Those last two points could have changed the sensor characteristics for high frequencies, but we are not sure.

The main uncertainty in the reciprocity principle is the difference in wave shapes: the ones originating from a vibrating string will have the violin as its acoustical centre, the excitation waves of the measurements are plane waves, having its acoustical centre at large distance. However, comparing our results with results from other researches do not give rise to the thought that this will effect the measurements a lot.

6.1.2 Analysis

In this research, algorithms are developed to extract the violin body resonance from the measurement results. As was seen, those methods are very sensitive for the overall frequency response of the violin, forcing us to cut the frequency spectrum into three pieces. The cross-over frequencies are to be chosen by hand, which is a little arbitrary. Furthermore, differences between the modelled and real power spectrum of the violin are large, suspecting that this part is the weakest link in the research.

6.1.3 Reproduction

The reproduction part needed some small adaptations of the Modalys software, and this works very well. The speed of the program is not decreased noticeably, which keeps the door open for real-time implementation of the directivity. Unfortunately there was not enough time to make a longer tune in Modalys which could demonstrate the effect, but the first attempts are promising.

6.2 Future work

As this research is not finished yet, there are a lot of recommendations for future work to give.

6.2.1 Complex reproduction

The first involves the reproduction part. As the spatial Fourier transform of the pattern gives us complex coefficients, we could use those for the reproduction as well. For this, the signal processing unit of La Tim'ee will be extended with 4 extra filters per loudspeaker. The signals who correspond to the real part of the spherical harmonics are distributed to the old filters, and the imaginary part to the new filters. Now, as the real and imaginary part of a signal will be out of phase for 90° , the extra filters are the same as for the real values, but they have a 90° phase shift for all frequencies. The extra 4 channels of output from Modalys can be generated the same as for the real values, so we will have a directivity matrix with 8 columns instead of 4.

6.2.2 More instruments

Another thing could be, to do the measurements and analysis on other instruments, and building with these a directivity pattern. A slightly different approach would be, to measure the directivity of all basic structures which are used in Modalys, and extending all those objects with directivity.

6.2.3 Rotating violin

One thing we did not take into account in the reproduction, was that in real life a violinist moves, or walks around. This will give a changing directivity pattern, not only in frequency, but also in time. This behaviour we can not reproduce, since we use a static directivity matrix in the synthesis. An algorithm can be written to change the directivity matrix during the synthesis, but further thought should be given. This might be implemented in a real-time version of the reproduction.

6.2.4 High frequency behaviour

As we have seen in the subsequent graphs, the high frequency behaviour of the violin can not be described well with low order harmonics. We have thought of two different solutions.

A first method, which is done by accident in our reproduction, is to use the spatial aliasing effect. The reproduction laws state, that to produce a dipole, the distance between two actuators should be smaller than the wavelength in air. This law will give a high frequency limit to the reproduction of the sound. By forcing La Tim'ee to produce frequencies above its aliasing frequency, we will get a random directivity pattern. Although this pattern will not fit the one from the violin at all, it will produce a directional behaviour with higher order spherical harmonics.

The second method would be to reproduce higher order spherical harmonics, needing a lot more work: for the zeroth and first order we needed 6 loudspeakers and 24 filters, but for the

second order, 6 more loudspeakers are needed, and a subsequent 72 filters (making $9 \cdot 12$ in total). The size of those loudspeakers should be kept small, in order to maintain the high frequency limit due to spatial aliasing. The effect of this extension can be modelled with the Matlab toolbox, the same way as done in this research for the zeroth and first order harmonics.

Chapter 7

Social report

Almost all the french people whom met in Paris, got a smile on their face when I said I did my internship at IRCAM. Although the institut has only one open week per year, a lot of people seem to have visited the institut. Why is this? It might be its [overkoepelend orgaan], the Centre Pompidou, which is known all over the world for its cultural habitat. The institut is located at a stone throw from the main building of Centre Pompidou, underneath the Fountains of the Birds by Niki de Saint-Phalle and Jean Tinguely. It will better be the main interest of a lot of people: Music! At the IRCAM research department, some hundred scientist work together in a lot of different fields: instrumental acoustics, Room acoustics, Musical perception and cognition, Analysis and Synthesis, Music representations, Real-time applications and Sound design.

- IRCAM as very hightech Institute
- highest priority of spreading the knowledge through papers or education
- enough budget to achieve hightech, at least 1 computer per person, different fast(!) computers for research
- internationally based: students and Ph.D.'s from all over the world
- Lots of cooperation in European projects
- Working env: Flexible hours, 24/24, nice collegues for the needed relaxation
- Paris: great town



Figure 7.1: Me on the early morning in the Anechoic Room.

Bibliography

- [1] Thomas SAUTREAU, Reproduction du rayonnement à l'aide d'une source multi haut-parleurs, Septembre 1997. Intern Report IRCAM.
- [2] Arnaud LABORIE, Capture échantillonnage et manipulations de fonctions de directivité. Application à l'enregistrement de scènes sonores 3D avec un micro SoundField. Octobre 2000. Mastère Spécialisé E.N.S.T., Report IRCAM.
- [3] Jean Marie ADRIEN, The Missing Link: Modal synthesis. Ch. 8 of Representations of Musical Signals, edited by G. DE POLI, A. PICCIALI, C. ROADS; MIT Press, 1991. ISBN 0-262-04113-8.
- [4] Francisco IOVINO, René CAUSSE, Richard DUDAS, Recent work around Modalys and Modal Synthesis. Internal Report IRCAM, 1997(?).
- [5] Jean-Marc JOT, Laurent CERVEAU, Olivier WARUSFEL, Analysis and synthesis of room reverberation based on a statistical time-frequency model. Internal Report IRCAM.
- [6] Philippe DÉROGIS, Analyse des vibrations et du rayonnement de la table d'harmonie d'un piano droit et conception d'un système de reproduction du champ acoustique. Thèse de doctorat, l'Université du Maine, 1997.
- [7] Matti KARJALAINEN, Jyri HUOPANIEMI, Vesa VALIMAKI, Direction-Dependent Physical Model of Musical Instruments. 15th International Congress on Acoustics (ICA '95), Trondheim Norway, June 26-30, 1995.
- [8] Gabriel WEINREICH, Eric B. ARNOLD, Method for measuring acoustic radiation fields. Journal Acoust. Soc. Am. 68 (2), August 1980.
- [9] Gabriel WEINREICH, Sound hole sum rule and the dipole moment of the violin. Journal Acoust. Soc. Am. 77 (2), Februari 1985.
- [10] Gabriel WEINREICH, Radiativity revisited; theory and experiments ten years later. Stockholm Music Acoustics Conference (SMAC) 1993, Taberg. Royal Swedish Academy of Music, no. 79 pp. 432-437.
- [11] Gabriel WEINREICH, Directional tone color. Journal Acoust. Soc. Am. 101 (4), April 1997.
- [12] Neville H. FLETCHER, Thomas D. ROSSING, The physics of Musical Instruments. Springer-Verlag, New York USA 1991.
- [13] Rozenn NICOL, Etude de la restitution du son spatialisé dans une zone étendue: Application à la téléprésence. Thèse, intern report at IRCAM, 1999.
- [14] David J. GRIFFITHS, Introduction to Quantum Mechanics. Prentice Hall 1995.

- [15] K. STEIGLITZ and L.M. BRIDE, A technique for the identification of linear systems.
- [16] Laboratoire d'Acoustique Musical, www.lam.jussieu.fr. Topics mentioned under supervision of Charles BESNAINOU.
- [17] W.Th. WENCKEBACH, Essentials of Semiconductor Physics. Wiley and Sons New York, USA, 2000.
- [18] Kenneth D. MARSHALL, Modal analysis of a violin. J. Acoust. Soc. Am, Vol. 77, No. 2, February 1985.
- [19] Carleen M. HUTCHINS, Virginia BENADE, Research Papers in Violin Acoustics 1975-1993. Acoustical Society of America, 1997.
- [20] George A. KNOTT, A modal analysis of the violin using MSC/NASTRAN and PATRAN. Thesis for Naval Postgraduate school, Monterey, California. 1987, [19] p. 507.